Light Scattering Study of the Formation and Structure of Partially Hydrolyzed Poly(acrylamide)/Calcium(II) Complexes

Shufu Peng[†] and Chi Wu*[,†,‡]

Department of Chemistry, The Chinese University of Hong Kong, Shatin, Hong Kong, and The Open Laboratory of Bond-selective Chemistry, Department of Chemical Physics, University of Science and Technology of China, Hefei, Anhui, China

Received June 9, 1998; Revised Manuscript Received October 1, 1998

ABSTRACT: The Ca^{2+} concentration and hydrolysis degree [$-COO^-$] dependence of the self-complexation of partially hydrolyzed poly(acrylamide) (HPAM) chains in $CaCl_2$ aqueous solution was systematically investigated by a combination of static and dynamic laser light scattering. We have, for the first time, revealed a transition between the intrachain and interchain complexations. For each given HPAM sample, there exists a critical Ca^{2+} concentration ($[Ca^{2+}]_{agg}$) at which the interchain HPAM complexation becomes dominant. $[Ca^{2+}]_{agg}$ is related to [$-COO^-$] by $[Ca^{2+}]_{agg} = 7.46 \times 10^{-9}$ $[-COO^-]^{-1.4}$, indicating that the complexation is not stoichiomeric and many Ca^{2+} ions are free in water. We also found that even at $[Ca^{2+}] > [Ca^{2+}]_{agg}$, the complexation at the initial stage was mainly an intrachain process, but gradually evolved into an interchain aggregation. The length of the initial stage increases as [$-COO^-$] and $[Ca^{2+}]$ decrease. Our results showed that in the complexation process, the weight average molecular weight (M_w) of the HPAM/Ca^{2+} complexes is scaled to the size (R) of the complexes as $M_w \propto R^{2.11\pm0.04}$ for different $[Ca^{2+}]$ and [$-COO^-$], suggesting that the HPAM/Ca^{2+} complexes have a fractal structure. The fractal dimension of 2.11 ± 0.04 shows that the complexation is a reaction-limited cluster aggregation (RLCA) process.

Introduction

The complexation of polyelectrolytes has been extensively studied.[1−4] It is known that certain metal ions like Ca^{2+} can specifically interact with carboxylic groups. If the carboxylic groups are attached to a polymer chain backbone, such as partially hydrolyzed poly(acrylamide) (HPAM), the interaction could lead to a chain aggregation through the polyion/metal "complexation".[5] Flory and Osterheld[6] showed, as early as 1954, that Ca^{2+} ions could change the chain conformation. Ohmine et al.[7] and Ben Jar et al.[8] studied the effects of monovalent and divalent cations on the collapsing of HPAM. Moreover, several attempts[9−11] have been made to describe the polyelectrolytes aggregation in terms of a few mechanistic models. Michaeli[12] interpreted the polyelectrolytes aggregation as a function of the ionization degree and of the inert monovalent electrolyte concentration in terms of a stoichiomeric complex between divalent cations and anionic groups.

The aggregation kinetics has also been extensively studied.[13] The observation that some colloidal clusters have fractal structures has sparked a renewed interest in the aggregation kinetics.[14] Two distinct aggregation kinetic processes have been proposed and investigated. One is the diffusion-limited cluster aggregation (DLCA) controlled by the time taken for two clusters to collide via Brownian diffusion,[15,16] and the other is the reaction-limited cluster aggregation (RLCA) in which the probability of forming a bond upon collision of two clusters is so high that the aggregation rate is chemically limited by its reaction rate. The RLCA has been observed in several colloid systems and modeled by computer simulation.[17−20] In general, the fractal dimension d_f is defined as $M \sim R^{df}$, where M is the molar mass and R is the cluster size.[16] In RLCA, $d_f \sim 1.55$ and ~ 2, respectively, in 2-dimensional and hierarchical 3-dimensional simulations. The experimental values of d_f for the clusters formed in RLCA were $\sim 2.1 \pm 0.1$. Ball et al.[21] pointed out that in RLCA, the slightly larger experimental d_f values were due to the cluster's polydispersity.

Laser light scattering (LLS) has been proved to be a particular useful method to study the aggregation process, especially in a very dilute solution in which a conventional viscometer does not has enough sensitivity. LLS is also a direct method to study fractal structures on the basis of the scattered intensity and the size dependence of the molar mass. It is worth noting that it is not trivial to prove a fractal structure, and the fractal concept has been abused in some cases. In this study, the complxation of the HPAM chains in $CaCl_2$ aqueous solution was investigated. We focused on (1) the transition from the intrachain HPAM complex to the interchain aggregation over a wide range of the hydrolysis degrees and Ca^{2+} concentrations and (2) the structure of the HPAM/Ca^{2+} complexes.

Experimental Section

Sample Preparation. The ultrapure acrylamide from Beijing Chemical Reagent Co. was further purified by a three-time recrystalliation. Poly(acrylamide) (PAM) was synthesized in water by a radical polymerization procedure detailed before.[22] The resultant PAM sample was hydrolyzed in 10% NaOH and 10% $NaCO_3$ aqueous solution at 60 °C.[23] The hydrolysis was controlled by the reaction time. The hydrolysis degree (HD%) of five partially hydrolyzed poly(acrylamide) (HPAM) samples was in the range 4.7−17.9% which were determined by titration with a 0.10N HCl standard solution.[24] The complexation was induced by adding dropwise a proper amount of dust-free $CaCl_2$ aqueous solution into ~2 mL of dust-free HPAM aqueous solution. The initial concentration of the HPAM solution was kept at 1.00×10^{-5} g/mL except otherwise specified. The resistivity of the deionized water used

[†] The Chinese University of Hong Kong.
[‡] University of Science and Technology of China.

10.1021/ma9809031 CCC: $18.00
Published on Web 01/14/1999

Table 1. Summary of LLS Results of Poly(acrylamide) and Partially Hydrolyzed Poly(acrylamide) in 1 N NaCl Aqueous Solution at 25 °C

sample	HD (%)	$M_w/10^6$ (g/mol)	$A_2/10^{-4}$ (mol·mL/g^2)	$\langle R_g\rangle$/nm	D/(cm^2/s)	$\langle R_h\rangle$/nm	$\langle R_g\rangle/\langle R_h\rangle$	$\mu_2/\langle\Gamma^2\rangle$
PAM	~0.0	2.20	1.57	105	3.29	74.2	1.41	0.19
HPAM1	4.7	2.05	2.96	117	3.03	80.9	1.45	0.19
HPAM2	8.1	1.96		117	3.05	80.2	1.46	0.19
HPAM3	10.8	1.98		113	3.07	79.5	1.43	0.20
HPAM4	14.0	1.82		112	3.16	77.1	1.45	0.17
HPAM5	17.9	1.66	6.65	119	2.97	82.3	1.45	0.20

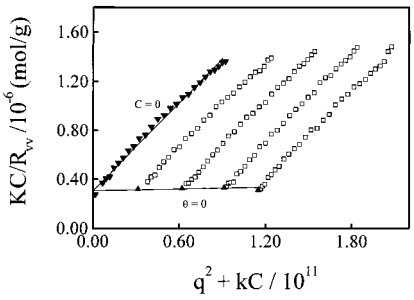

Figure 1. Typical Zimm plot for poly(acrylamide) in 1 N NaCl aqueous solution at 25 °C.

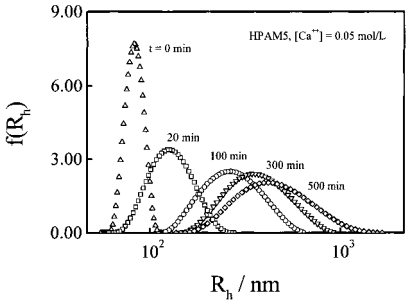

Figure 2. Time dependence of the hydrodynamic radius distribution $f(R_h)$ of the HPAM/Ca^{2+} complexes for the self-complexation of the HPAM chains in 0.05 M $CaCl_2$ aqueous solution.

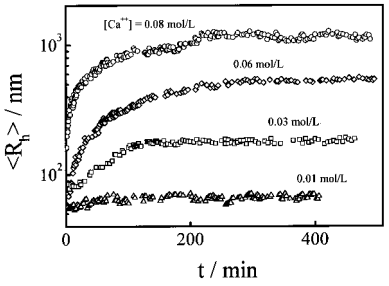

Figure 3. Time dependence of the average hydrodynamic radius $\langle R_h\rangle$ of the HPAM/Ca^{2+} complexes for the self-complexation of the HPAM chains in different $CaCl_2$ aqueous solutions.

in this study was 18.3 MΩ cm. All the HPAM solutions used in LLS were clarified with a 0.5 μm Millipore filter, and the $CaCl_2$ aqueous solution was clarified with a 0.1 μm Whatman filter (Anotop 25) in order to remove dust.

Laser Light Scattering. In static LLS, we were able to obtained the weight-average molar mass M_w, the second-order virial coefficient A_2, and the z-average radius of gyration $\langle R_g^2\rangle_z^{1/2}$ (or written as $\langle R_g\rangle$) of the polymer chains from the angular dependence of the excess absolute scattering intensity, known as the Rayleigh ratio $R_{vv}(q)$, on the basis of[25,26]

$$\frac{KC}{R_{vv}(q)} = \frac{1}{M_w}\left(1 + \frac{1}{3}\langle R_g^2\rangle q^2\right) + 2A_2C \qquad (1)$$

where $K = 4\pi n^2(dn/dC)^2/N_A\lambda_0^4$, and $q = (4\pi n/\lambda_0)\sin(\theta/2)$, with n, dn/dC, λ_0, and θ being the solvent refractive index, the specific refractive index increment, the wavelength of the light in vacuo, and the scattering angle, respectively. For PAM and HPAM in 1 N NaCl aqueous solutions at 25 °C, $[dn/dC]_{532.8\ nm} = 0.175$ and 0.146 mL/g, respectively.

In dynamic LLS, the cumulant analysis of the measured intensity-intensity time correlation function $G^{(2)}(t,q)$ of a dilute polymer solution can lead to the average characteristic line width $\langle\Gamma\rangle$.[27,28] For a diffusive relaxation, Γ is related to the average translational diffusion coefficient D by $D = (\Gamma/q^2)_{q\to 0}$, and D is the further related to the hydrodynamic radius R_h by $R_h = k_BT/(6\pi\eta D)$ with k_B, η, and T being the Boltzmann constant, the solvent viscosity, and the absolute temperature, respectively. On the other hand, the Laplace inversion of $G^{(2)}(t,q)$, e.g., the CONTIN program,[29] can directly lead to the line width distribution $G(\Gamma)$ or the hydrodynamic radius distribution $f(R_h)$. The LLS instrumentation has been detailed before.[30]

Results and Discussion

Individual PAM and HPAM chains (i.e., unimer) were first characterized. Figure 1 shows a typical Zimm plot of PAM in 1 N NaCl aqueous solution at 25 °C, where C ranges from 3.17×10^{-5} to 1.15×10^{-4} g/mL. The values of M_w, $\langle R_g\rangle$, and A_2 calculated on the basis of eq 1 are summarized in Table 1. The decrease of M_w as the hydrolysis degree (HD%) increases indicates a slight degradation of the PAM chains in the hydrolysis process. The positive values of A_2 indicated that 1 N NaCl aqueous solution is a good solvent for both PAM and HPAM at 25 °C. The ratios of $\langle R_g\rangle/\langle R_h\rangle \sim 1.5$ are expected for linear flexible polymer chains in a good solvent.

Figure 2 shows the time dependence of the self-complexation of the HPAM chains in 0.05 M $CaCl_2$ aqueous solution in terms of the change of the hydrodynamic radius distribution $f(R_h)$. It clearly shows that the increases of the size and the distribution width with time. Figure 3 shows the time dependence of the average hydrodynamic radius $\langle R_h\rangle$ of the HPAM/Ca^{2+} complexes after the addition of different amounts of Ca^{2+}, where $\langle R_h\rangle = \int f(R_h)R_h\, dR_h$. Note that for each given Ca^{2+} concentration, there exists a plateau value $\langle R_h\rangle_{max}$. Figure 3 clearly shows that for a given HPAM sample, both the initial complexation rate $[d\langle R_h\rangle/dt]_{t\to 0}$ and $\langle R_h\rangle_{max}$ increase with the Ca^{2+} concentration, which is understandable because Ca^{2+} acts as the cross-linking agent to interconnect ("complex") the HPAM chains. It is worth noting that when $[Ca^{2+}] < 0.01$ M, $\langle R_h\rangle$ was nearly independent of time, indicating that there exists a critical Ca^{2+} concentration for the interchain complexation. Figure 4 shows that $[d\langle R_h\rangle/dt]_{t\to 0} \propto [Ca^{2+}]^2$, indicating that, for a given HPAM sample, the initial rate of the self-complexation is strongly dependent on $[Ca^{2+}]$.

Figure 5 shows the complexation kinetics in terms of the change of $\langle R_h\rangle$ for five different HPAM samples in a given $CaCl_2$ aqueous solution. For each HPAM sample, $\langle R_h\rangle$ approaches a plateau $\langle R_h\rangle_{max}$. As expected, $\langle R_h\rangle_{max}$ decreases as the hydrolysis degree decreases. It is interesting to note that, in Figure 4, there exists an initial stage in which $\langle R_h\rangle$ *decreases*, which reveals an

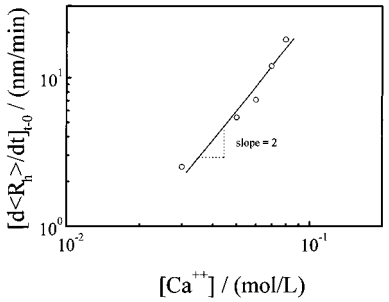

Figure 4. Ca^{2+} concentration dependence of the initial complexation rate $[d\langle R_h\rangle/dt]_{t\to 0}$ calculated from the data in Figure 3, where the slope of the line is 2.

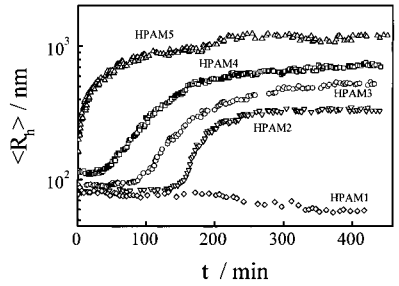

Figure 5. Time dependence of the average hydrodynamic radius $\langle R_h\rangle$ of the HPAM/Ca^{2+} complexes for the self-complexation of HPAM samples in 0.08 M $CaCl_2$ aqueous solution.

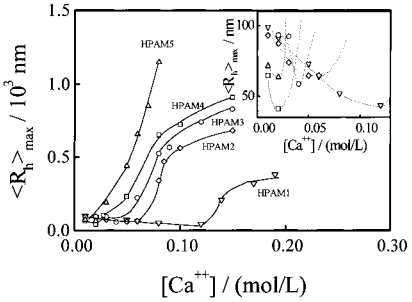

Figure 6. Ca^{2+} concentration dependence of the maximum average hydrodynamic radius $\langle R_h\rangle_{max}$, where $\langle R_h\rangle_{max}$ is the plateau value as shown in Figure 3.

intrachain complexation in which individual HPAM chains contract before the interchain aggregation. For HPAM5, the *interchain* complexation was dominant and the initial stage was too short to be observed, while for HPAM1, the *intrachain* complexation was dominant, so that no increase of $\langle R_h\rangle$ was observed. As for HPAM2, HPAM3, and HPAM4, the transition from the *intrachain* complexation to *interchain* complexation is very clear. To our knowledge, this transition is observed and reported for the first time. Figure 5 reveals that for a given Ca^{2+} concentration, the *interchain* complexation is directly related to the hydrolysis degree because the carboxylic groups act as "stickers" to complex with the HPAM chains, similar to the results of the PMA/Ca^{2+} system reported by Yuko et al.[31]

Figure 6 shows the Ca^{2+} concentration dependence of $\langle R_h\rangle_{max}$ for five different HPAM samples. The inset shows an enlargement of the low $[Ca^{2+}]$ range in which $\langle R_h\rangle_{max}$ decreases as $[Ca^{2+}]$ increases, indicating the *intrachain* complexation. Figure 6 shows that at higher $[Ca^{2+}]$ concentrations, $\langle R_h\rangle$ increases sharply as $[Ca^{2+}]$ increases, revealing a Ca^{2+}-induced transition between the *intrachain* and *interchain* complexations. The $[Ca^{2+}]$ concentration at which $\langle R_g\rangle$ starts to increases is defined as the aggregation concentration $[Ca^{2+}]_{agg}$.

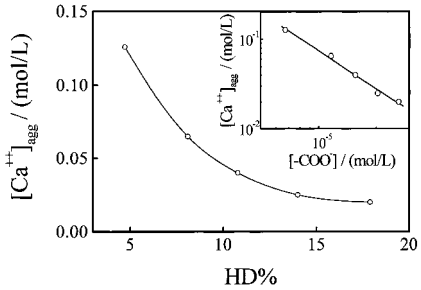

Figure 7. Hydrolysis degree (HD%) dependence of the aggregation concentration ($[Ca^{2+}]_{agg}$), where $[Ca^{2+}]_{agg}$ was defined to be the Ca^{2+} concentration at which $\langle R_h\rangle$ starts to increase as shown in Figure 6. The inset shows a double logarithmic plot of $[Ca^{2+}]_{agg}$ vs $[-COO^-]$ and the straight line represents a least-squares fit of $[Ca^{2+}]_{agg} = 7.46 \times 10^{-9}\,[-COO^-]^{-1.4}$.

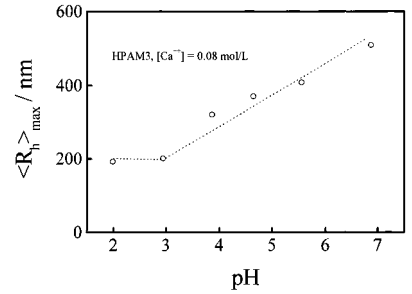

Figure 8. pH dependence of the maximum average hydrodynamic radius $\langle R_h\rangle_{max}$ for a given ratio of $[Ca^{2+}]/[-COO^-]$.

Figure 7 shows the hydrolysis degree (HD%) dependence of $[Ca^{2+}]_{agg}$, where the inset shows a double logarithmic plot of $[Ca^{2+}]_{agg}$ vs $[-COO^-]$. The line in the inset shows a least square fitting of $[Ca^{2+}]_{agg} = 7.46 \times 10^{-9}\,[-COO^-]^{-1.4}$. Figures 3 and 5 clearly reveal that increasing either the hydrolysis degree or $[Ca^{2+}]$ can promote the *interchain* complexation. Figure 7 shows that increasing the hydrolysis degree is more effective, but there is an upper limit of ~20% beyond which the increases of HD% have less effect on the *interchain* complexation. The ratio of $[-COO^-]/[Ca^{2+}]$ should be 2 if every Ca^{2+} ion in the solution complexes with two $-COO^-$ ions. But, as shown in Figure 7, $[-COO^-]/[Ca^{2+}]$ is much smaller than 2, indicating that most of Ca^{2+} ions are free in water.

Figure 8 shows the pH dependence of $\langle R_h\rangle_{max}$ for a given $[Ca^{2+}]$ concentration. Note that $K_{acid} \equiv [-COO^-][H^+]/[COOH]$ and pH $\equiv -\log[H^+]$, i.e., $\log [-COO^-]/[COOH] = \log(K_{acid}) + pH$, where K_{acid} is a constant. Therefore, $[-COO^-]/[COOH]$ increases as pH increases. In other words, the effective hydrolysis degree (or the "sticking" probability when two HPAM chains collide) increases with pH. This is why $\langle R_h\rangle_{max}$ of the HPAM/Ca^{2+} complexes increases with pH. When pH < 3, $\langle R_h\rangle_{max}$ becomes independent on pH, which can be attributed to the shift of $-COO^-$ to $-COOH$, so that further complexation of the HPAM chains stops.

From Figures 3−8, we know that the complexation between the HPAM chains in $CaCl_2$ aqueous solution could be dominated by either the *intrachain* or *interchain* complexation, depending on the hydrolysis degree and Ca^{2+} concentration. The complexation can be viewed as follows: each HPAM is a long coil chain with hundreds of "stickers" ($-COO^-$). Two "stickers" and one Ca^{2+} ion can be driven thermodynamically together to form one $(-COO)_2Ca$ complex point. The *interchain* "points" result in the clustering of the HPAM chains.

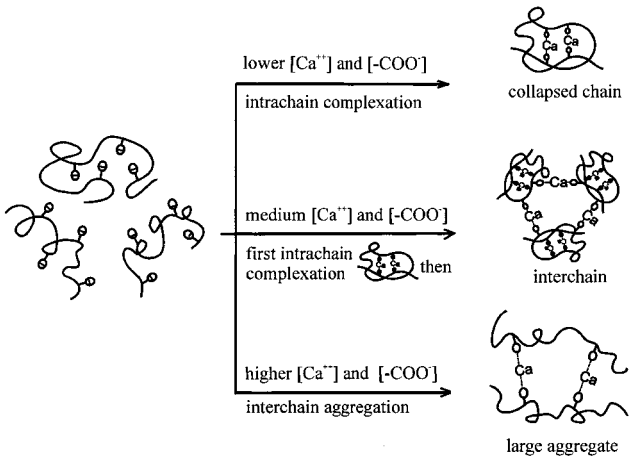

Figure 9. Schematic of the self-complexation of the HPAM chains under different experimental conditions.

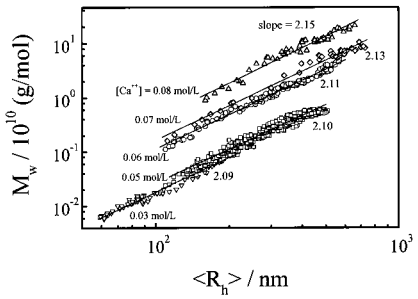

Figure 10. Double logarithmic plots of the weight average molar mass (M_w) vs the average hydrodynamic radius $\langle R_h \rangle$ for the HPAM5 chains in the presence of different amounts of Ca^{2+} ions.

These clusters further collide with each other or with individual HPAM chains, leading to larger clusters. Finally, when either Ca^{2+} ions or $-COO^-$ groups are consumed, the complexation stops. In the process, clusters with different size were formed as shown in Figure 2. Note that the *intrachain* $-COO^-$ groups are closer than those *interchain* $-COO^-$ groups. For the HPAM chains with a low hydrolysis degree in the presence of small amounts of Ca^{2+} ions, the *intrachain* complexation is expected to be easier, while in the case of a high hydrolysis degree and a high Ca^{2+} concentration, the *interchain* complexation becomes dominant, as shown schematically in Figure 9. In the medium range of $[Ca^{2+}]$ and $[-COO^-]$, the HPAM chains first undergo the *intrachain* complexation through the neighboring carboxylic acid groups on the same chain before the *interchain* complexation becomes apparent.

Figure 10 shows double logarithmic plots of the weight average molar mass (M_w) of the HPAM/Ca^{2+} complexes vs their average hydrodynamic radius $\langle R_h \rangle$ for a given HPAM sample but different Ca^{2+} concentrations. Figure 11 shows double logarithmic plots of M_w vs $\langle R_h \rangle$ for a given Ca^{2+} concentration but different HPAM samples, where the values of M_w were calculated from the measured Rayleigh ratio on the basis of eq 1. It should be stated that the ratio of $\langle R_g \rangle / \langle R_h \rangle$ was close to a constant of ~1.35 in the measurable range of $\langle R_g \rangle$. Figures 10 and 11 clearly demonstrate that M_w can be scaled to $\langle R_h \rangle$, i.e., $M_w \propto \langle R \rangle^{2.11 \pm 0.04}$, for different Ca^{2+} concentration and different HPAM samples. This suggests that the HPAM/Ca^{2+} complexes have a fractal structure with a dimension of $d_f = 2.11 \pm 0.04$, which

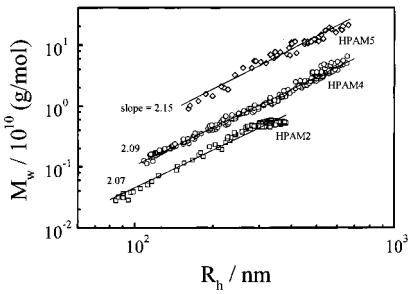

Figure 11. Double logarithmic plots of the weight average molar mass (M_w) of the vs the hydrodynamic radius $\langle R_h \rangle$ for different HPAM samples in 0.08 M $CaCl_2$ aqueous solution.

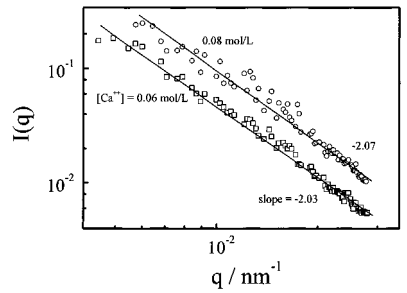

Figure 12. Double logarithmic plots of the scattering intensity $I(q)$ vs the scattering vector q for the HPAM5 chains in two different $CaCl_2$ aqueous solutions after the maximum complexation was reached.

is in a good agreement with the value predicated for RLCA.[32,33]

Figure 12 shows double logarithmic plots of the scattering intensity $I(q)$ vs the scattering vector q after the maximum complexation was reached. The slope of ~ 2 also indicates that the HPAM/Ca^{2+} complexes have a fractal structure.

In summary, a systematic study of the self-complexation of partially hydrolyzed poly(acrylamide) (HPAM) chains in $CaCl_2$ aqueous solution at 25 °C shows, for the first time, that there is a transition between the intrachain and interchain complexations. The complexation can be well controlled by both the hydrolysis degree and Ca^{2+} concentration. For a given HPAM sample, there exists a Ca^{2+} concentration ($[Ca^{2+}]_{agg}$) at which the interchain complexation becomes dominant and the size of the complexes increases as $[Ca^{2+}]$ increases. On the other hand, for a given Ca^{2+} concentration, the size of the complexes increases as the hydrolysis degree increases. The HPAM/Ca^{2+} complexes have a fractal structure with a dimension of 2.11 ± 0.04, indicating that the self-complexation is a reaction-limited cluster aggregation process.

Acknowledgment. The financial support of this work by the RGC (the Research Grants Council of Hong Kong Government) Earmarked Grants 1997/98 (CUHK4181/97P, 2160082) and the National Distinguished Young Investigator Fund (1996) are gratefully acknowledged. S.P. is grateful for the generous financial support of The Lee Hysan Foundation Limited for her stay at the CUHK.

References and Notes

(1) Dautzenberg, H. *Macromolecules* **1997**, *30*, 7810.
(2) Bekturov, E. A.; Bimendina, L. A. *Advances in Polymer Science;* Springer: Berlin, Heidelberg, Germany, and New York, 1981; Vol. 41, p 99.

(3) Tsuchida, E.; Abe, K. *Advances in Polymer Science*; Springer: Berlin, Heidelberg, Germany, and New York, 1992; Vol. 45.
(4) Zhang, Y. B.; Xiang, M. L.; Jiang, M.; Wu, C. *Macromolecules* **1997**, *30*, 2035.
(5) Jordan, D. S.; Green, D. W.; Terry, R. E.; Willhite, G. P. *J. Soc. of Pet. Eng.* **1982**, *8*, 463.
(6) Flory, P. J.; Osterheld, J. E. *J. Phys. Chem*. **1954**, *58*, 653.
(7) Ohmine, I.; Tanaka, T. *J. Chem. Phys*. **1982**, *77*, 5725.
(8) Ben Jar, P. Y.; Wu, Y. S. *Polymer* **1997**, *38*, 2557.
(9) Ikegami, A.; Imai, N. J. *Polym. Sci*. **1962**, *56*, 133.
(10) Dubin, P., Bock, J.; Davies, R. M.; Schulz, D. N.; Thies, C. *Macromolecular Complexes in Chemstry and Biology*: Springer-Verlag: Berlin, 1994.
(11) Narh, K. A.; Keller, A. *J. Polym. Sci., Part B: Polym. Phys*. **1993**, *31*, 231.
(12) Michaeli, I. *J. Polym.Sci*. **1960**, *48*, 291.
(13) Family, F., Landau, D. P., Eds., *Kinetics of Aggregation and Gelation*; North-Holland: Amsterdam, 1984.
(14) Burns, J. L.; Yan, Y. D.; Jameson, G. J.; Biggs, S. *Langmuir* **1997**, *13*, 6413.
(15) Kolb, M.; Botet, R.; Jullien, R. *Phys. Rev. Lett*. **1983**, *51*, 1123.
(16) Meakin, P. *Phys. Rev. Lett*. **1983**, *51*, 1119.
(17) Von Schulthess, G. K.; Benedek, G. B.; Deblois, R. W. *Macromolecules* **1980**, *13*, 939.
(18) Schaefer, D. W.; Martin, J. E.; Wiltzius, P.; Cannell, D. S. *Phys. Rev. Lett*. **1984**, *52*, 2371.
(19) Jullien, R.; Kolb, M. *J. Phys*. **1984**, *A17*, L693.
(20) Brown, W. D.; Ball, R. C. *J. Phys*. **1982**, *A18*, L517.
(21) Ball, R. C.; Weitz, D. A.; Written, T. A.; Leyvraz, F. *Phys. Rev. Lett*. **1987**, *58*, 274.
(22) Ji, H. J.; Sun, Z. W.; Zhang, W. X.; Li, Z. H. *Acta Polym. Sin*. **1994**, *11*, 559.
(23) Tanaka, T.; Nishio, I.; Ueno-Nishio, S. T. *Science* (*Washington, D.C.*) **1982**, *218*, 467.
(24) Ji, L. Y.; Zhang, X. M.; Ha, R. H. *Polym. Mater. Sci. Eng*. **1995**, *11*, 122.
(25) Debye, P. J. *Phys. Colloid Chem*. **1947**, *51*, 18.
(26) Zimm, B. H. *J. Chem. Phys*. **1948**, *16*, 1099.
(27) Pecora, R. *Dynamic Light Scattering:* Plenum Press: New York, 1976.
(28) Chu, B. *Laser Light Scattering*, 2nd ed.; Academic Press: New York, 1991.
(29) Provencher, S. W. *Makromol.Chem*. **1979**, *180*, 201.
(30) Wu, C.; Zhou, S. Q. *Macromolecules* **1995**, *28*, 8381.
(31) Yuko, I.; Michael, B.; Manfred, S.; Klaus, H. *Macromolecules* **1998**, *31*, 728.
(32) Martin, T. A.; Joost, H. J.; Van Opheusden, X. *Phys. Rev. E* **1996**, *53*, 5044.
(33) Lin, M. Y.; Lindsay, H. M.; Weitz, D. A.; Ball, R. C.; Klein, R.; Meakin, P. *Phys. Rev*. **1990**, *41*, 2005.

MA9809031